Wet-spinning of TEMPO-oxidized Lignocellulose Nanofibrils and Functionalization of the Filament with Ag Nanoparticles

Chan-Woo Park,[a] Rajkumar Bandi,[a] Ramakrishna Dadigala,[a] Song-Yi Han,[a] Jeong-Ki Kim,[b] Gu-Joong Kwon,[a,c] Nam-Hun Kim,[a,b] and Seung-Hwan Lee [a,b,c,*]

Wet spinning was studied for lignocellulose nanofibrils (TOLCNF) obtained by TEMPO oxidation and mechanical defibrillation of deep eutectic-like solvent-treated lignocellulose. First, the morphological characteristics, water retention value, and specific surface area of the TOLCNF were studied. The effects of the TOLCNF concentration (1.5, 2.0, and 2.5 wt%) and spinning rate (0.1, 1.0, and 10 mL/min) on the wet-spun filament diameter, orientation index, and tensile properties were studied. With an increase in the TOLCNF concentration, the average diameter increased, whereas the orientation index and tensile strength decreased. An increased spinning rate resulted in an increased orientation index and tensile strength but a decrease in the average diameter. To further extend their applicability, Ag nanoparticles (AgNPs) were grown *in situ* on the filament surface using UV irradiation. Spherical AgNPs with diameters of 30 to 90 nm were observed using scanning electron microscopy. An increased AgNP content improved the tensile strength and elastic modulus of the filaments.

DOI: 10.15376/biores.18.1.505-517

Keywords: Wet-spinning; Lignocellulose nanofibrils; Silver nanoparticles; UV irradiation

*Contact information: a: Institute of Forest Science, Kangwon National University, Chuncheon 24341, Republic of Korea; b: Department of Forest Biomaterials Engineering, College of Forest and Environmental Sciences, Kangwon National University, Chuncheon 24341, Republic of Korea; c: Kangwon Institute of Inclusion Technology, Kangwon National University, Chuncheon 24341, Republic of Korea; *Corresponding author: lshyhk@kangwon.ac.kr*

INTRODUCTION

Cellulose has been used in the form of long filaments in the textile industry. The filaments are generally manufactured by wet-spinning cellulose dissolved in solvents, and it is known as regenerated cellulose fiber (Nishiyama *et al*. 2019; Sayyed *et al*. 2019). Viscose and Lyocell rayon, as regenerated cellulosic fibers, are the most representative commercially produced fibers obtained from natural fiber sources (Ramamoorthy *et al*. 2015; Lundahl *et al*. 2017). To produce viscose rayon, cellulose dissolved in 16 to 19% sodium hydroxide is first treated with carbon disulfide, which results in the generation of sodium cellulose xanthate. Viscose rayon is obtained by wet-spinning xanthate dissolved in a solution of 2 to 5% sodium hydroxide and regeneration in sulfuric acid. Instead of derivatizing cellulose, the Lyocell technique simply dissolves cellulose in an organic solvent, *i.e.* N-methylmorpholine N-oxide (NMMO). Dry-jet wet spinning across an air gap to accomplish drawing before regeneration is used to create lyocell filaments. Consequently, lyocell filaments frequently exhibit better mechanical performance than

viscose filaments. Nevertheless, these production procedures are quite energy-intensive and environmentally hazardous, especially when attempting to recover wasted solvents (Sayyed *et al*. 2019).

Natural cellulosic fibers typically have micron-sized diameters and short initial lengths (10 to 65 mm). Furthermore, these fibers must be yarned to be spun into a long filament (Walther *et al*. 2011; Kafy *et al*. 2017; Lundahl *et al*. 2017). However, the strength of the natural yarn fiber is lower than that of the regenerated cellulosic fiber because of the poor connection between the fibers. Recently, the fabrication of high-strength long filaments from natural cellulose, particularly from cellulose nanofibrils (CNF, which are also called nanofibrillated cellulose), through wet spinning has gained considerable attention (Iwamoto *et al*. 2011; Kafy *et al*. 2017; Lundahl *et al*. 2017). CNF are highly dispersible in water with high viscosity, making wet spinning extremely suitable for filament production. Furthermore, wet-spun filaments have excellent mechanical properties, such as a tensile strength of 100 to 400 MPa and an elastic modulus of 7 to 10 GPa (Iwamoto *et al*. 2011; Kafy *et al*. 2017; Lundahl *et al*. 2017). The properties of CNF filaments are affected by various factors, such as the cellulose source, chemical composition, and process parameters (Lundahl *et al*. 2017). Hence, it is interesting to explore new types of CNF for wet spinning. Furthermore, multifunctional filaments can be obtained by the functionalization of CNF.

Typically, silver nanoparticles (AgNPs) are clusters of Ag atoms of 1 to 100 nm in size. Owing to their high surface-to-volume ratio, AgNPs exhibit superior electrical, catalytic, and optical properties compared to bulk silver (Han *et al*. 2020). Owing to their superior physical and chemical characteristics, high conductivity, good catalytic performance, and wide range of antimicrobial activities, AgNPs have attracted significant attention (Kim *et al*. 2009; Bandi *et al*. 2020; Reddy *et al*. 2021). Reportedly, AgNPs not only improve the mechanical properties of wet-spun filaments but also endow the filament with antimicrobial activities. This is expected to expand the range of applications of wet-spun filaments.

This study aimed to explore the wet-spinning capability of new type of CNF and synthesis of AgNPs on wet-spun filaments to improve their functionality. CNFs were prepared by TEMPO-mediated oxidation of Korean red pine treated with choline chloride/lactic acid (1/1) at 130 °C and pristine cellulose. The wet-spun filaments were fabricated from the prepared CNFs via wet-spinning, and AgNPs were synthesized on the filaments by Ag+ reduction via UV irradiation. The dependence of the properties of the wet-spun filaments on the spinning conditions and AgNP content was examined.

EXPERIMENTAL

Materials

Lignocellulose pretreated with choline chloride/lactic acid (mole ratio 1:1)-based deep eutectic-like solvent (DES) at 130 °C for 24 h (lignin content: 3.6%, hemicellulose content: 4.7%) and commercial pristine cellulose powder (W50) were used for the CNF preparation. TEMPO, sodium bromide, 30% sodium hypochlorite solution, 50% NaOH solution, HCl, and acetone were purchased from Daejung Chemical & Metals (Republic of Korea) and were used without further purification.

CNF Preparation

One gram of pristine cellulose powder or DES-treated lignocellulose was suspended in 100 mL of deionized water (DW). Then, 0.016 g of TEMPO and NaBr (0.1 g) were dissolved in the suspension and stirred for 1 h. The TEMPO oxidation reaction was initiated by adding 3.5 mL of 12% $NaClO_2$. The pH of the suspension was maintained at 10 by adding 0.5 M NaOH using an autotitrator (TitroLine easy, SI Analytics, Germany). The reaction was conducted for approximately 3 to 5 h until no more NaOH was consumed. Finally, 5 mL of ethanol was added to quench the reaction, and the suspension pH was adjusted to 7 by adding 0.1 mM HCl. The obtained residue was washed with DW using a vacuum pump and diluted to 0.1 wt.%.

The suspension was defibrillated using a high-pressure homogenizer (MN400BF; PICOMAX, Seoul, Korea) at an operating pressure of 20,000 psi (1.38 MPa) for 5 passes. The CNFs prepared from the DES-treated lignocellulose and pristine cellulose were named TOLCNF and TOCNF, respectively.

Carboxyl Content Calculation

Carboxyl content was calculated using conductivity titration method (Gu *et al.* 2015). At first, 1 mL of 0.1 N HCl was added to a 50 mL of 0.1 wt% CNF suspension to protonate the carboxyl groups. Then the suspension was titrated against 0.02 M NaOH solution. During titration the conductivity values were recorded and plotted against the NaOH volume. Carboxyl content was determined using the following equation,

$$Carboxyl\ content\ (mmol\ per\ gram\ of\ nanofibril) = \frac{cv}{m} \quad (1)$$

where c is the NaOH concentration (0.02 M), v is the volume of NaOH consumed in the plateau region of the plot and m is the CNF dry weight (0.05 g)

Water Retention Value (WRV)

A polytetrafluoroethylene (PTFE) membrane filter (pore size: 0.2 μm) was placed on a glass filter (pore size: 10 μm) and embedded in 50 mL centrifugation tube. The CNF suspensions were put on the membrane filters, then centrifuged at 2,000 × g for 15 min in a swing rotor. As obtained CNF pancake was carefully removed from PTFE membrane filter. The samples were dried at 105 °C to a constant weight. The WRV was calculated with the following equation,

$$\text{WRV } (\%) = (m_1\text{-}m_2)/m_2 \times 100 \quad (2)$$

where m_1 is the LCNF weight after centrifugation and m_2 is the weight of the dried sample.

Specific Surface Area

The CNF suspension was put into a centrifuge tube and centrifuged for 20 minutes at 40,000 g, with the supernatant decanted. Then, using a vortex mixer, tert-butyl alcohol was put into the centrifuge tube and blended with the sediment. To eliminate water and maintain the nanoscale shape of CNF, the solvent exchange process was done 15 times. After centrifugation, the samples were freeze-dried for 12 hours at -55 °C. With N_2 adsorption at 77 K, the specific surface area of the LCNFs was evaluated using a Brunauer-Emmett-Teller (BET) analyzer (BELSORP-Max, BEL Japan Inc., Japan).

Preparation of Wet-spun Filament

The CNF concentrations were adjusted to 1.5, 2.0, and 2.5 wt% by centrifugation. The CNF suspensions were laced in a syringe with a needle of 24 G (outer diameter: 0.56 mm; inner diameter: 0.30 mm) and wet-spun in acetone at spinning rates of 0.1, 1.0, and 10 mL/min. After removal from acetone, the filaments were immersed in $AgNO_3$ solutions of 0.1, 1.0, and 3.0 mM concentrations. Then, the filaments were rinsed with DW and UV-irradiated (RX-H1000D, Raynics Co., Korea) with a 1,000 W UV lamp for 15 min to reduce Ag^+ to Ag^0.

Morphology Observation

The morphology of the CNFs was observed using atomic force microscopy (AFM) (Nanoscope 5, Bruker, Karlsruhe, Germany). The samples for AFM observations were prepared as follows. First, a freshly cleaved mica disk was immersed in 0.1% polyethyleneimine solution for 10 min and dried under ambient conditions at room temperature. The CNF suspension (0.05%) was dropped on a mica disk and spin-coated using a spin coater (ACE-200, Dong-ah Trade, Republic of Korea) for 1 min at 3,000 rpm. The wet-spun filaments were coated with iridium using a high-vacuum sputter coater (EM ACE600; Leica Microsystems, Ltd., Germany). The morphologies were observed using SEM at an accelerating voltage of 1 kV. Energy dispersive X-ray spectroscopy (EDS) analysis was conducted at an accelerating voltage of 15 kV in mapping mode.

Tensile Testing

The filaments were placed in a thermo-hygrostat at a relative humidity of 65% to minimize the influence of variations in the relative humidity on the tensile properties. The tensile properties were measured using a load cell of 5 N at a crosshead speed of 3 mm/min with a span length of 10 mm. Five specimens of each sample were tested, and the average values were reported.

Two-dimensional XRD (2D XRD)

The orientation of the wet-spun filament was analyzed using 2D XRD (Bruker D8 Discover with a Vantec 500 detector; Bruker). A CuKα radiation source at 40 kV and 40 mA was used, and 2D XRD analysis was performed with a beam diameter of 1.0 mm in the transmission mode 70 mm from the detector. Forty filaments were bundled together to obtain sufficient intensity. From the 2D XRD data, the orientation index (α) of the CNFs in the wet-spun filament was calculated by azimuthal breath analysis using Eq. 1,

$$\alpha = (180 - \beta c)/180 \quad (3)$$

where βc is the half width of the azimuthal direction of the equatorial reflection of the (200) plane obtained from the 2D XRD patterns.

RESULTS AND DISCUSSION

Table 1 lists the characteristics of both TOLCNF and TOCNF, including the recovery yield, diameter, carboxyl content, water retention value, and specific surface area. The yields of the water-insoluble TOLCNF and TOCNF were 85.9% and 91.1%, respectively. The carboxyl content of TOCNF was 1.54 mmol/g, which is higher than that of TOLCNF (1.41 mmol/g). These results may be attributed to the presence of lignin in the

TOLCNF. TEMPO oxidation is selectively performed on the C6 primary hydroxyl groups of cellulose so that TEMPO oxidation does not occur on lignin. Moreover, the dissolution of lignin in NaBr and NaClO solutions may lead to a decrease in the recovery yield and carboxyl content (Ma *et al*. 2012). Kuramae *et al*. (2014) investigated the effect of hemicellulose content in holocellulose on TEMPO oxidation (Kuramae *et al*. 2014). The carboxyl content and recovery yield were attributed to the cellulose content, not the hemicellulose content, because hemicellulose in holocellulose can be degraded to water-soluble compounds during the TEMPO oxidation process. The morphological characteristics of the TOLCNF and TOCNF, as revealed by AFM analysis, are shown in Fig. 1. Both TOLCNF and TOCNF have diameters of 4 to 6 nm and lengths on the micrometer scale. Similar to TOCNF, the water retention value and specific surface area of TOLCNF were 594% and 217 m^2/g, respectively.

Table 1. Recovery Yield, Carboxyl Content, Diameter, Water Retention Value, and Specific Surface Area of TOLCNF and TOCNF

Sample	Recovery Yield (%)	Carboxyl Content (mmol/g)	Diameter (nm)	Water Retention Value (%)	Specific Surface Area (m^2/g)
TOLCNF	85.9	1.41	4-6	594	217
TOCNF	91.1	1.54	4-6	586	239

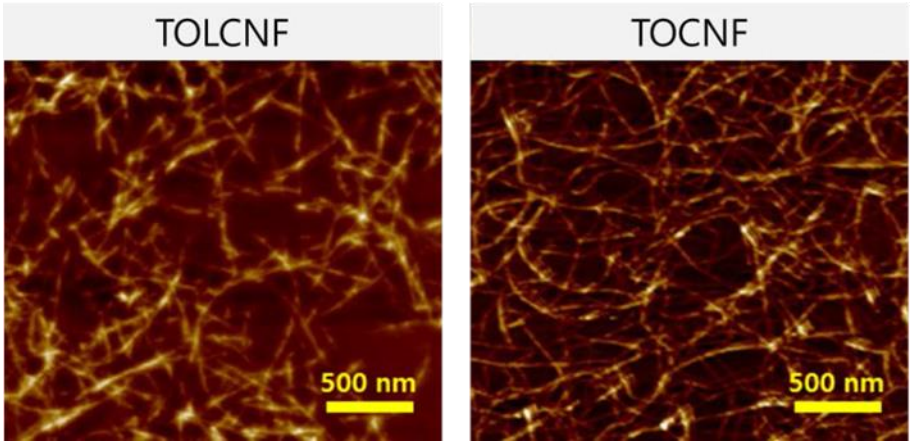

Fig. 1. AFM images of TOLCNF and TOCNF

Figure 2 shows the morphological characteristics of the wet-spun filaments made of TOLCNF and TOCNF under different spinning conditions. In all samples, aggregated CNFs with a high aspect ratio were observed on the wet-spun filaments. The densities and average diameters of the filaments under different spinning conditions are summarized in Table 2. The density was 1.4 to 1.5 g/cm^3. In filaments made of both TOLCNF and TOCNF, the average diameter decreased with an increasing spinning rate. Increasing the CNF concentration increased the average diameter. Park *et al*. (2020) reported that the properties of wet-spun filaments depend on the CNF concentration and spinning rate (Park *et al*. 2020). The average diameter decreased as the spinning rate and CNF concentration increased and decreased, respectively.

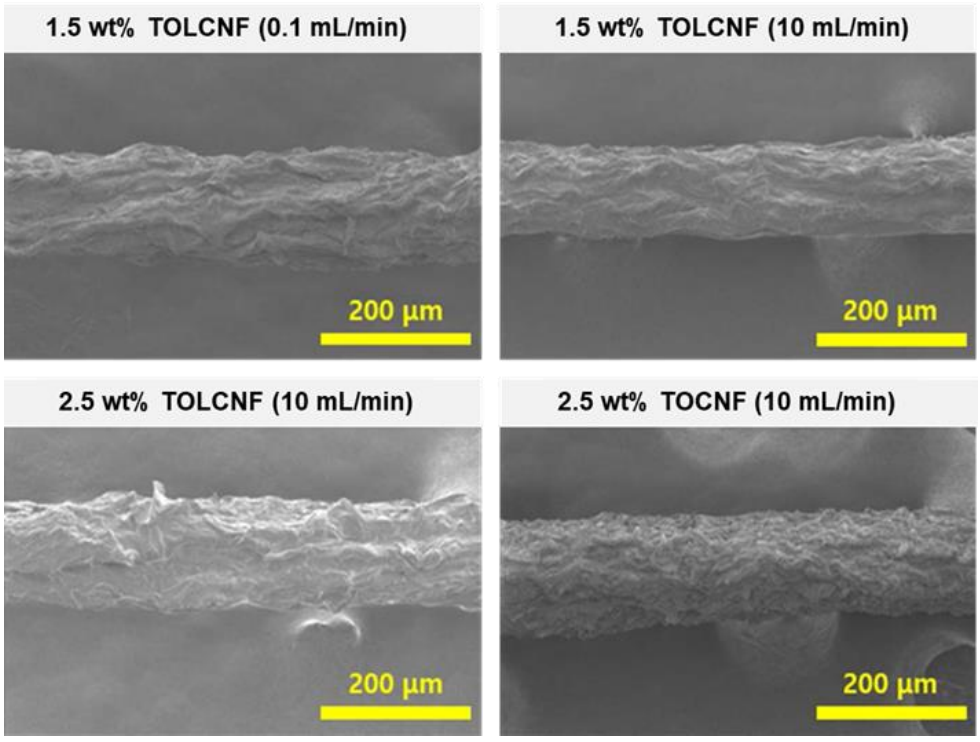

Fig. 2. SEM images of the wet-spun filaments made of TOLCNF and TOCNF with different spinning conditions

Table 2. Average Diameter, Density, and Orientation Index of the Wet-Spun Filaments Obtained from TOLCNF and TOCNF Using Different Spinning Conditions

Sample	Concentration (wt%)	Spinning Rate (mL/min)	Average Diameter (nm)	Density (g/cm^3)	Orientation Index
TOLCNF	1.5	0.1	202 ± 18	1.4	0.64
		1.0	195 ± 14	1.5	0.67
		10	190 ± 16	1.4	0.71
	2.0	10	203 ± 17	1.5	0.65
	2.5	10	210 ± 20	1.5	0.63
TOCNF	1.5	0.1	201 ± 15	1.4	0.64
		1.0	192 ± 14	1.5	0.68
		10	188 ± 12	1.5	0.70

Figure 3 shows the morphological characteristics and EDS analysis of the wet-spun filaments obtained from TOLCNF and TOCNF with AgNPs at different $AgNO_3$ concentrations. All samples contained AgNPs with diameters of 30 to 80 nm on the filaments. In the filament made of TOLCNF, the number of AgNPs on the filament increased with increasing $AgNO_3$ concentration. EDS analysis confirmed the presence of AgNPs on the filaments, and the atomic percentage of AgNPs was evaluated. The atomic percentage of AgNPs in the filament from TOLCNF increased from 2.68% to 5.52% with the increase in the $AgNO_3$ concentration from 0.1 to 3 mM. The filament obtained from TOCNF with 3 mM $AgNO_3$ contained 5.50% AgNPs.

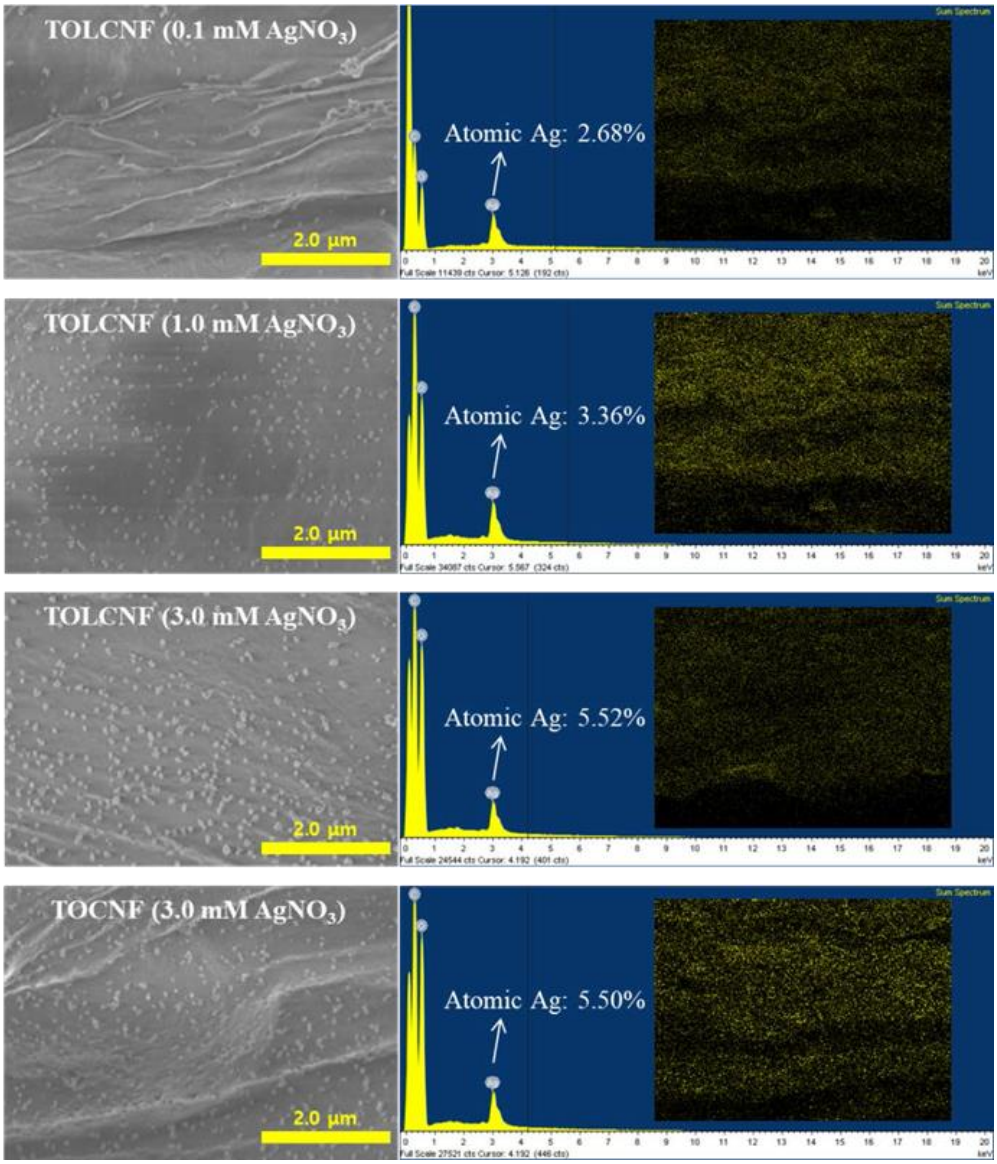

Fig. 3. Morphological characteristics and EDS analysis of wet-spun filaments with AgNPs obtained from TOLCNF and TOCNF at different AgNO3 concentrations

The dependence of AgNPs size on the filaments obtained from TOLCNF and TOCNF on the AgNO3 concentration was evaluated from the SEM images, with histograms of AgNPs sizes shown in Fig. 4. The AgNPs size in the filament obtained from TOLCNF increased with increasing $AgNO_3$ concentration from 0.1 to 3.0 mM. Volova *et al*. (2018) prepared BNC/AgNP films at 0.0001, 0.001, and 0.01 mM $AgNO_3$ under heating at 90 °C and reported similar results for the effect of the $AgNO_3$ concentration on the size of the AgNPs on the BNC film (Volova *et al*. 2018). The AgNPs obtained using higher $AgNO_3$ concentrations were larger. Pedroza-Toscano *et al*. (2017) also reported that the AgNPs reduced at 0.4 mM $AgNO_3$ on carboxymethyl cellulose (CMC) were larger than those reduced at 0.2 mM $AgNO_3$ (Pedroza-Toscano *et al*. 2017). Additionally, the AgNPs on the TOCNF filament with 3 mM AgNO3 were slightly smaller than those on the TOLCNF filament.

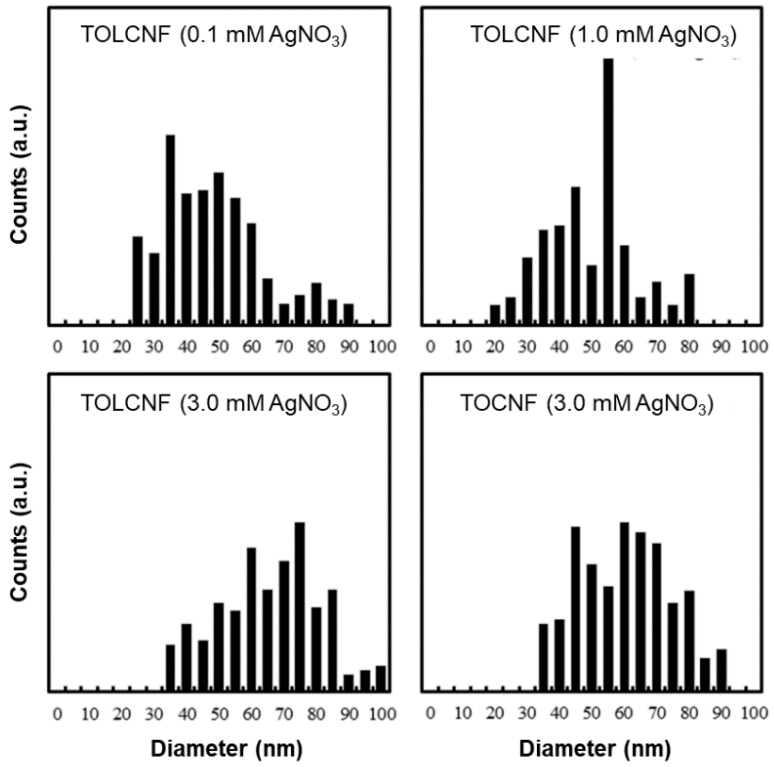

Fig. 4. Particle size distribution of the AgNPs on the filaments obtained from TOLCNF and TOCNF at different AgNO3 concentrations

Figure 5 shows the 2D XRD diffractograms and the relative intensity of the (200) plane along the azimuthal direction of the wet-spun filaments obtained from TOLCNF and TOCNF at concentrations of 1.5 to 2.5 wt.% and spinning rates of 0.1 to 10 mL/min. The diffractograms displayed a typical peak for cellulose I, corresponding to the (110) and (200) planes. A randomly fabricated cellulose film demonstrated ring patterns along the azimuthal angle in the 2D XRD diffractogram. In contrast, in the filament samples, the reflections were strong at the middle azimuth with two arc patterns because the TOLCNF and TOCNF were arranged along the axial direction of the filaments. The orientation index values of the filaments were calculated from the relative intensity of the (200) plane and are summarized in Table 2. The orientation index values of the filaments for 1.5 wt.% TOLCNF and TOCNF were 0.64 to 0.71 and 0.64 to 0.70, respectively, showing similar values. The orientation index values of both filaments increased with increasing spinning rate from 0.1 to 10 mL/min. An increase in the spinning rate may give rise to a stronger shearing force on the CNFs, promoting the orientation of the CNFs along the axial direction of the filament. Iwamoto *et al*. (2011) studied the effect of wet-spinning conditions on the properties of wet-spun filaments from CNF (Iwamoto *et al*. 2011). An increase in the spinning rate resulted in an increased orientation index in the wet-spun CNF filaments. In addition, the orientation index decreased with increasing concentration of the TOLCNF suspension at the same spinning rate of 10 mL/min. Park *et al*. (2020) also reported that the wet-spun filaments obtained from 2.5 wt.% and 3.5 wt.% HCNF had orientation index values of 0.67 and 0.60, respectively (Park *et al*. 2020). This may be because the higher concentration of TOLCNF increased the contact between the CNFs, and thus interfered with the orientation of the CNF induced by the shear force generated by the fluid flow.

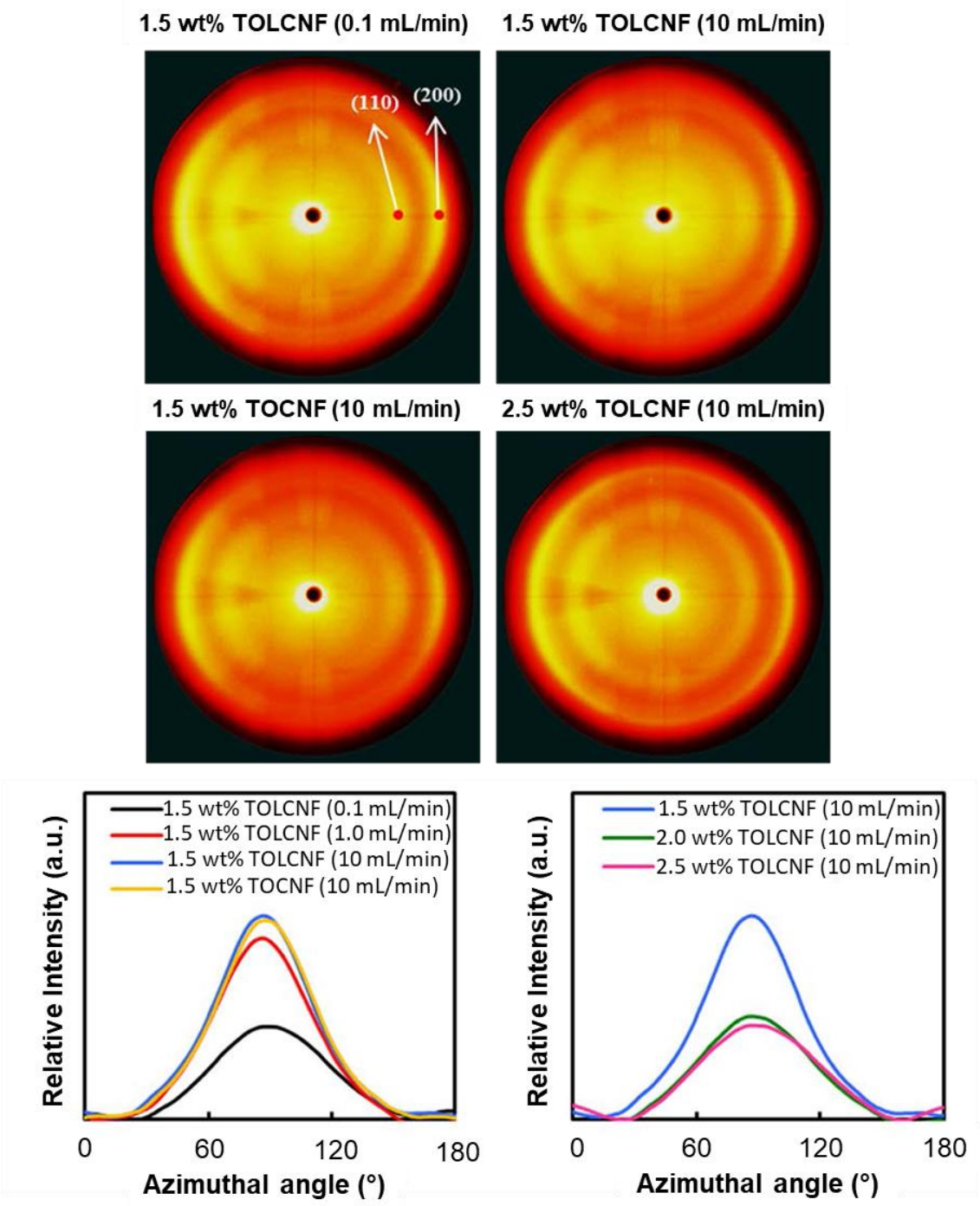

Fig. 5. 2D XRD diffraction patterns and azimuthal profiles of the (200) reflections of wet-spun filaments obtained from TOLCNF and TOCNF at different spinning conditions

Figure 6 shows the tensile strength, elastic modulus, and elongation at break measurements of the wet-spun filaments obtained from TOLCNF and TOCNF under different spinning conditions. Under the same spinning conditions, the tensile strength of the wet-spun filament made of TOLCNF with a lignin content of 3.6% was lower than that of the filament obtained from TOCNF. This can be attributed to the presence of hydrophobic lignin in the filaments. The lignin in the fiber weakened the hydrogen bonding between the nanofibrils, resulting in a decrease in the filament tensile strength. The

filament obtained from TOLCNF had a higher elastic modulus than that obtained from TOCNF. Park *et al*. (2020) reported that the wet-spun filament obtained from LCNF had a higher elastic modulus than the filaments obtained from HCNF and PCNF without lignin, whereas it had a lower tensile strength. For all the samples, an improvement in the tensile strength and elastic modulus was observed with an increasing spinning rate. As shown in Fig. 5 and Table 2, the increase in the orientation index was due to the increasing spinning rate. As the orientation increased, the cellulose crystals in the CNFs aligned along the fiber axis to enhance the mechanical properties. Deterioration in the tensile strength of the wet-spun filament obtained from TOLCNF was observed as the concentration increased from 1.5 to 2.5 wt.%, owing to the decreased value of the orientation index (Table 2). Lundahl *et al*. (2016) investigated the mechanical properties of wet-spun CNF filaments at different CNF concentrations (Lundahl *et al*. 2016). A lower concentration of CNF promoted nanofibril orientation, resulting in an improvement in the tensile strength and elastic modulus. The elongation at break of the wet-spun filament obtained from TOLCNF was in the range of 5 to 6%, which is lower than that of the filament obtained from TOCNF.

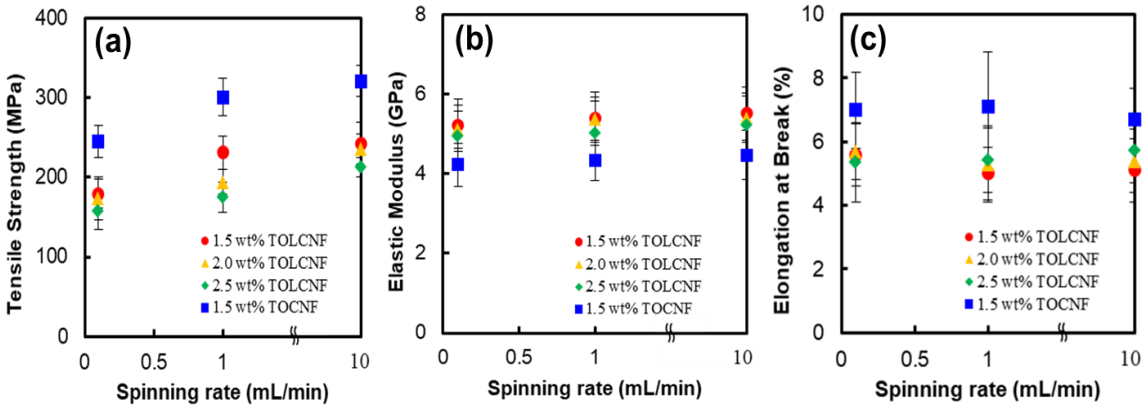

Fig. 6. Tensile strength, elastic modulus, elongation at break of wet-spun filaments obtained from TOLCNF and TOCNF at different spinning rates

Figure 7 shows the tensile strength, elastic modulus, and elongation at the break of the wet-spun filaments obtained from TOLCNF and TOCNF at different $AgNO_3$ concentrations. For all of the samples, an increase in the tensile strength and elastic modulus was observed with an increase in the $AgNO_3$ concentration from 0.1 to 3 mM. It was confirmed that AgNPs act as reinforcing fillers in the filaments. The AgNPs had a strong affinity for the hydroxyl and carboxyl groups in the TOCNFs. In addition, AgNPs could enhance the adhesion between the TOCNFs. For example, Raghavendra *et al*. (2013) prepared gum acacia or guar-gum-loaded cotton fibers with and without AgNPs and found that the presence of AgNPs in the fibers enhanced their tensile strength and elastic modulus (Raghavendra *et al*. 2013). Gollapudi *et al*. (2020) also reported the effects of AgNP synthesis on the properties of cotton fabrics (Gollapudi *et al*. 2020). With the increase in the $AgNO_3$ concentration, the tensile strength and elastic modulus of the cotton fabric with AgNPs also increased. Contrastingly, the elongation at the break did not show a significant dependence on the silver content. In summation, the filaments with small diameter and good tensile properties can possibly extend to textile application. Further the filaments with AgNPs can be used in making antimicrobial textiles and textile catalysts that can be used to remove organic pollutants.

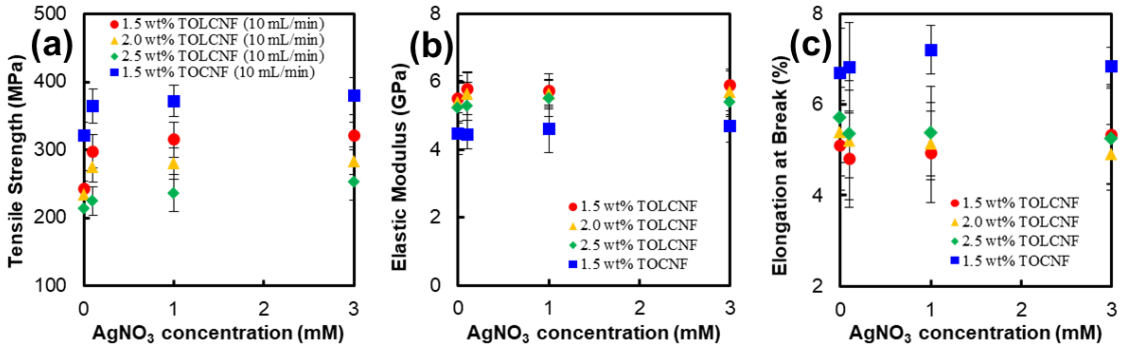

Fig. 7. Tensile strength, elastic modulus, and elongation at break values of the wet-spun filaments obtained from TOLCNF and TOCNF at different AgNO3 concentrations.

CONCLUSIONS

1. TEMPO-oxidized lignocellulose nanofibrils (TOLCNF) with average diameters of 4 to 6 nm were prepared from deep-eutectic-like solvent-treated lignocellulose.
2. Wet-spun filaments were successfully prepared from TOLCNF and characterized.
3. The average diameter of the wet-spun filaments decreased with increasing spinning rate and decreasing TOLCNF concentration.
4. The orientation index values calculated from 2D-X-ray diffraction increased with an increase in spinning rate and decrease in concentration.
5. The tensile strength of the fiber increased remarkably with increasing spinning rate, whereas a slight decrease was observed with increasing concentration.
6. Ag nanoparticles (AgNPs) were synthesized on filaments from 0.1 to 3.0 mM AgNO3 solutions using UV irradiation. Filament AgNP content increased with increasing $AgNO_3$ concentration.
7. AgNPs acted as a reinforcing filler in the filament, and the increased AgNP content improved the tensile strength and elastic modulus of the filaments.

ACKNOWLEDGMENTS

This research was supported by the Basic Science Research Program through the National Research Foundation of Korea (NRF), funded by the Ministry of Education (No. 2018R1A6A1A03025582).

REFERENCES CITED

Bandi, R., Alle, M., Park, C.-W., Han, S.-Y., Kwon, G.-J., Kim, J.-C., and Lee, S.-H. (2020). "Rapid synchronous synthesis of Ag nanoparticles and Ag nanoparticles/ holocellulose nanofibrils: Hg(II) detection and dye discoloration," *Carbohydrate Polymers* 240(April), article 116356. DOI: 10.1016/j.carbpol.2020.116356

Gollapudi, V. R., Mallavarapu, U., Seetha, J., Akepogu, P., Amara, V. R., Natarajan, H.

and Anumakonda, V. (2020). "*In situ* generation of silver and silver oxide nanoparticles on cotton fabrics using *Tinospora cordifolia* as bio reductant," *SN Applied Sciences* 2(3), 1-10. DOI: 10.1007/s42452-020-2331-1

Gu, J., and Hsieh, Y. L. (2015). "Surface and structure characteristics, self-assembling, and solvent compatibility of holocellulose nanofibrils," *ACS Applied Materials and Interfaces*, 7(7), 4192-4201. DOI: 10.1021/am5079489

Han, J.-K., Madhusudhan, A., Bandi, R., Park, C.-W., Kim, J.-C., Lee, Y.-K., Lee, S.-H., and Won, J.-M. (2020). "Green synthesis of AgNPs using lignocellulose nanofibrils as a reducing and supporting agent," *BioResources* 15(2), 2119-2132. DOI: 10.15376/biores.15.2.2119-2132

Iwamoto, S., Isogai, A., and Iwata, T. (2011). "Structure and mechanical properties of wet-spun fibers made from natural cellulose nanofibers," *Biomacromolecules* 12(3), 831-836. DOI: 10.1021/bm101510r

Kafy, A., Kim, H. C., Zhai, L., Kim, J. W., Hai, L., Van, Kang, T. J., and Kim, J. (2017). "Cellulose long fibers fabricated from cellulose nanofibers and its strong and tough characteristics," *Scientific Reports* 7(1), 1-8. DOI: 10.1038/s41598-017-17713-3

Kim, J., Kwon, S., and Ostler, E. (2009). "Antimicrobial effect of silver-impregnated cellulose: Potential for antimicrobial therapy," *Journal of Biological Engineering* 3, 1-9. DOI: 10.1186/1754-1611-3-20

Kuramae, R., Saito, T., and Isogai, A. (2014). "TEMPO-oxidized cellulose nanofibrils prepared from various plant holocelluloses," *Reactive and Functional Polymers* 85, 126-133. DOI: 10.1016/j.reactfunctpolym.2014.06.011

Lundahl, M. J., Cunha, A. G., Rojo, E., Papageorgiou, A. C., Rautkari, L., Arboleda, J. C., Rojas, O. J. (2016). "Strength and water interactions of cellulose I filaments wet-spun from cellulose nanofibril hydrogels," *Scientific Reports* 6(1), 1-13. DOI: 10.1038/srep30695

Lundahl, M. J., Klar, V., Wang, L., Ago, M., and Rojas, O. J. (2017). "Spinning of cellulose nanofibrils into filaments: A review," *Industrial and Engineering Chemistry Research* 56(1), 8-19. DOI: 10.1021/acs.iecr.6b04010

Ma, P., Fu, S., Zhai, H., Law, K., and Daneault, C. (2012). "Influence of TEMPO-mediated oxidation on the lignin of thermomechanical pulp," *Bioresource Technology* 118, 607-610. DOI: 10.1016/j.biortech.2012.05.037

Nishiyama, Y., Asaadi, S., Ahvenainen, P., and Sixta, H. (2019). "Water-induced crystallization and nano-scale spinodal decomposition of cellulose in NMMO and ionic liquid dope," *Cellulose* 26(1), 281-289. DOI: 10.1007/s10570-018-2148-x

Park, C. W., Park, J. S., Han, S. Y., Lee, E. A., Kwon, G. J., Seo, Y. H., Gwon, J. G., Lee, S. Y., and Lee, S. H. (2020). "Preparation and characteristics of wet-spun filament made of cellulose nanofibrils with different chemical compositions." *Polymers* 12(4), 949. DOI: 10.3390/POLYM12040949

Pedroza-Toscano, M. A., López-Cuenca, S., Rabelero-Velasco, M., Moreno-Medrano, E. D., Mendizabal-Ruiz, A. P., and Salazar-Peña, R. (2017). "Silver nanoparticles obtained by semicontinuous chemical reduction using carboxymethyl cellulose as a stabilizing agent and its antibacterial capacity," *Journal of Nanomaterials* 2017. DOI: 10.1155/2017/1390180

Raghavendra, G. M., Jayaramudu, T., Varaprasad, K., Sadiku, R., Ray, S. S., and Mohana Raju, K. (2013). "Cellulose-polymer-Ag nanocomposite fibers for antibacterial fabrics/skin scaffolds," *Carbohydrate Polymers* 93(2), 553-560. DOI: 10.1016/j.carbpol.2012.12.035

Ramamoorthy, S. K., Skrifvars, M., and Persson, A. (2015). "A review of natural fibers used in biocomposites: Plant, animal and regenerated cellulose fibers," *Polymer Reviews* 55(1). DOI: 10.1080/15583724.2014.971124

Reddy, G. B., Dadigala, R., Bandi, R., Seku, K., Kotewararao, D., Magatayaru, K. G., and Shalan, A. (2021). "Microwave-assisted preparation of a silver nanoparticles/N-doped carbon dots nanocomposite and its application for catalytic reduction of rhodamine B, methyl red and 4-nitrophenol dyes," *RSC Advances* 11(9), 5139-5148. DOI: 10.1039/D0RA10679H

Sayyed, A. J., Deshmukh, N. A., and Pinjari, D. V. (2019). "A critical review of manufacturing processes used in regenerated cellulosic fibres: Viscose, cellulose acetate, cuprammonium, LiCl/DMAc, ionic liquids, and NMMO based lyocell," *Cellulose* 26, 2913-2940. DOI: 10.1007/s10570-019-02318-y

Volova, T. G., Shumilova, A. A., Shidlovskiy, I. P., Nikolaeva, E. D., Sukovatiy, A. G., Vasiliev, A. D., and Shishatskaya, E. I. (2018). "Antibacterial properties of films of cellulose composites with silver nanoparticles and antibiotics," *Polymer Testing* 65, 54-68. DOI: 10.1016/j.polymertesting.2017.10.023

Walther, A., Timonen, J. V. I., Díez, I., Laukkanen, A., and Ikkala, O. (2011). "Multifunctional high-performance biofibers based on wet-extrusion of renewable native cellulose nanofibrils," *Advanced Materials* 23(26), 2924-2928. DOI: 10.1002/adma.201100580

Article submitted: October 4, 2022; Peer review completed: November 1, 2022; Revised version received and accepted: November 10, 2022; Published: November 16, 2022.
DOI: 10.15376/biores.18.1.505-517